

## **Supplementary Methods**

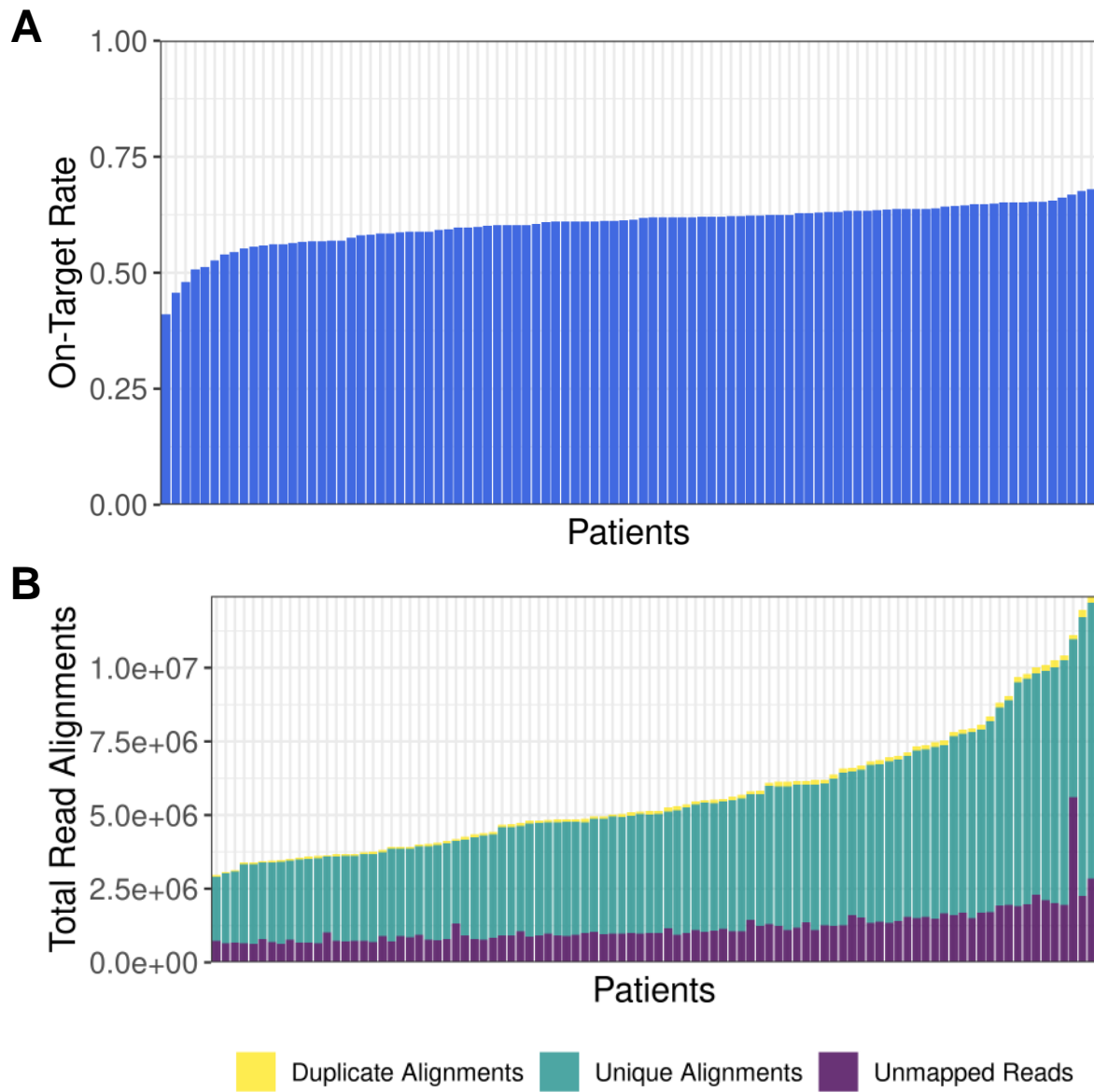
### **Description of real-world prostate cancer databank used for study**

We have developed a prospectively collected, clinically annotated, real-world prostate cancer biobanks and datasets, using uniform standard operating procedures (SOPs) applied to all blood sample acquisitions that mitigate the effects of pre-analytic bias. All SOPs include a uniform blood-based collection of specimens in patients visiting Huntsman Cancer Institute (HCI). Prostate cancer patients receiving treatments are approached under institutional biospecimen collection IRB-approved study of “Total Cancer Care” (*IRB# 00089989; IRB# 00139755*) and written informed consent is obtained. Collection of blood is performed under Clinical Laboratory Improvement Amendments (CLIA) supervision of the Biorepository and Molecular Pathology (BMP) Core facility at HCI and routed to the investigator’s research lab for uniform processing. All collections used in this study are performed in EDTA tubes and plasma generated from platelet-poor fractions used for proteomic analyses and processing is completed within two hours of collection and banked in -80°C and with no freeze-thaws. Granular clinical annotation is obtained from electronic medical records (EMRs) with data dictionaries.

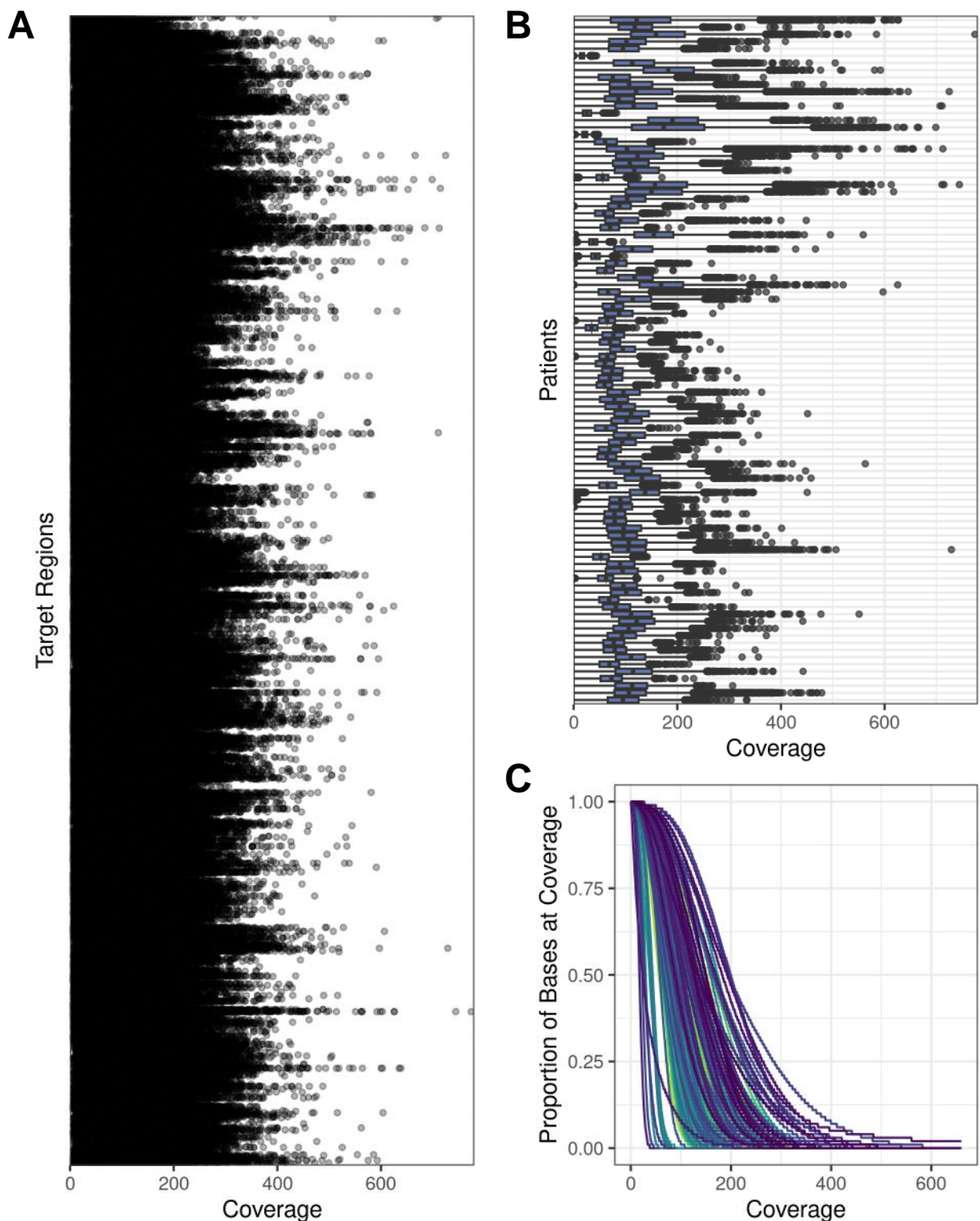
### **Blood collection and cfDNA extraction**

Whole blood collected in 4.5 mL EDTA tubes from all patients in the biobank was subjected to centrifugation at 2000 rpm for 10 minutes and a second centrifugation of the supernatant at 3000 rpm for 10 minutes to make platelet-poor plasma. 0.5-1 mL fractions of the plasma samples were stored at -80 °C until use. 1-2 mL of plasma was used for automated cfDNA extraction with the Maxwell RSC ccfDNA Plasma Kit (Promega, #AS1480). cfDNA quantification was performed using Qubit.

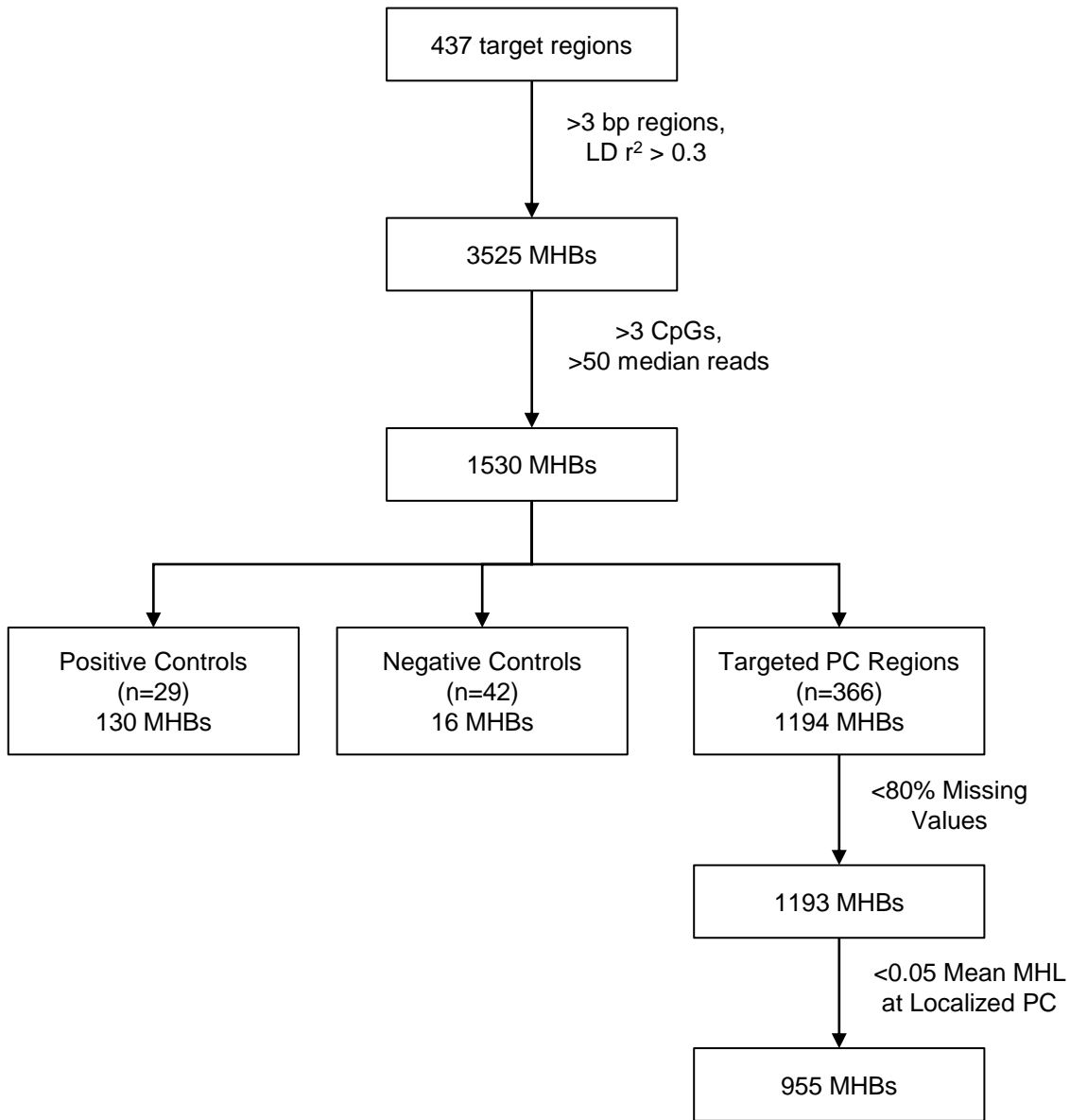
## Supplementary Figures



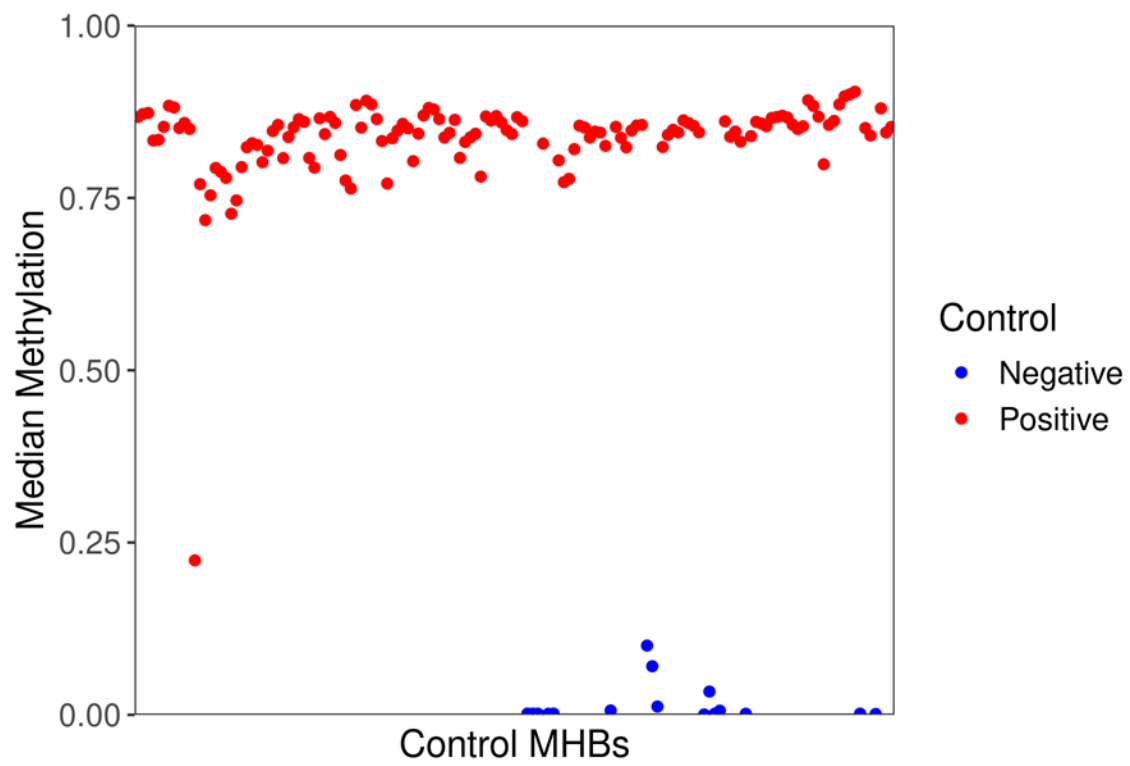
**Supplementary Figure S1: Distribution of on-target rate and total read alignments across patients. (A)** Distribution of on-target rate across each patient sample (n=96) **(B)** The composition of all alignments, consisting of unmapped reads, unique alignments, and duplicate alignments for each patient.



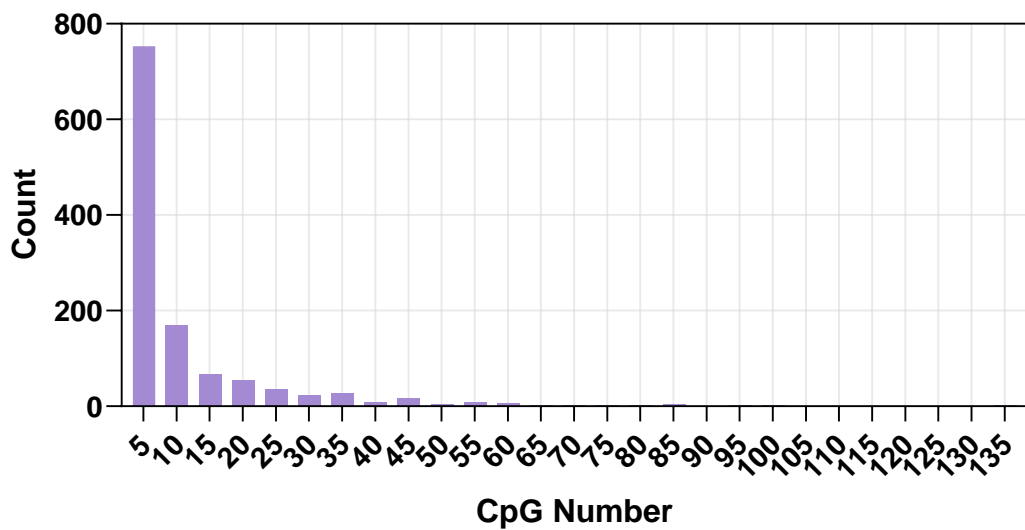
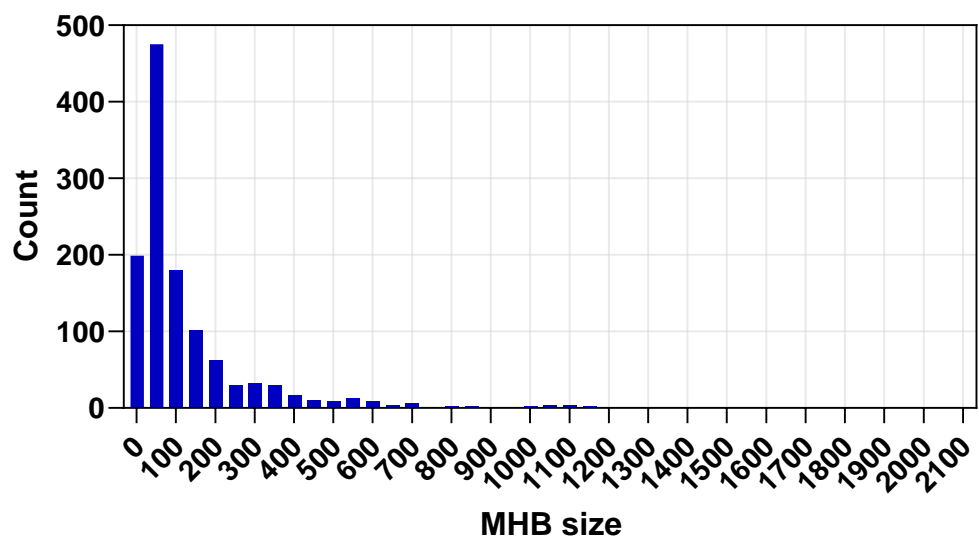
**Supplementary Figure S2: Sequencing coverage across target regions and patients.** (A) The coverage of each target region (n=437) across all patients (n=96). (B) The coverage of target regions across each patient. (C) Cumulative distribution of proportion of bases covered for a given coverage value across the target regions.



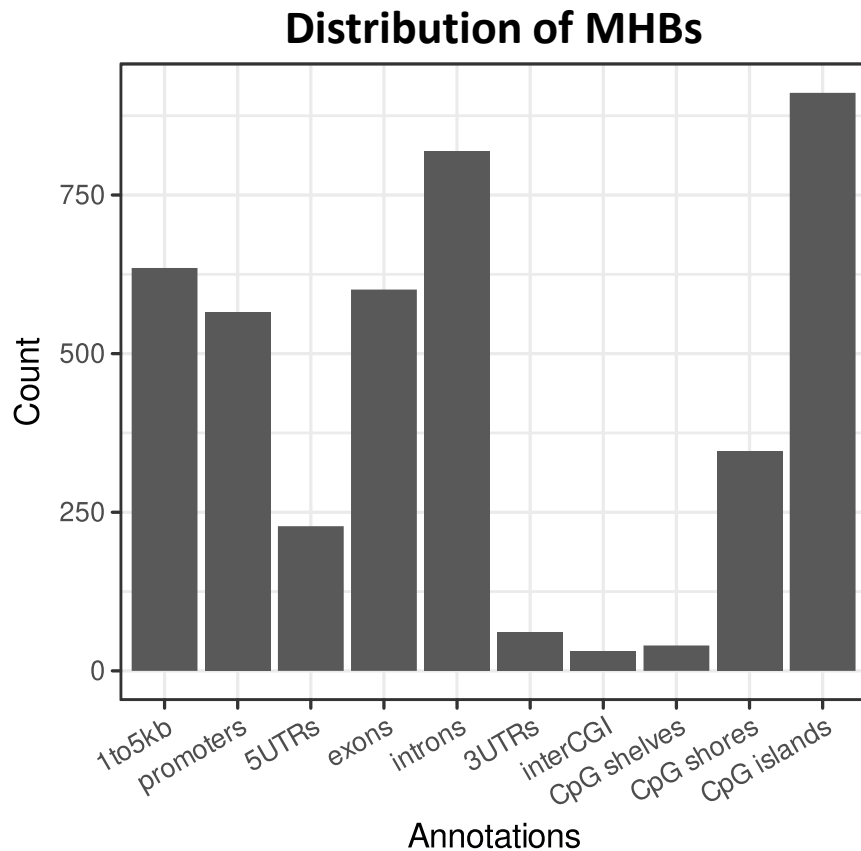
**Supplementary Figure S3: Identification of methylation haplotype blocks from target regions.**  
 MHBs were identified from target regions and filtered to identify regions with sufficient read counts (>50 median reads) and CpGs (>3 CpGs) within targeted prostate cancer regions. MHBs within the targeted PC regions were further filtered to retain MHBs with sufficient data (<80% missing values) and hypomethylated mean MHL (<0.05) at the localized PC state. *PC* prostate cancer, *MHBs* methylation haplotype blocks, *MHL* methylation haplotype load.



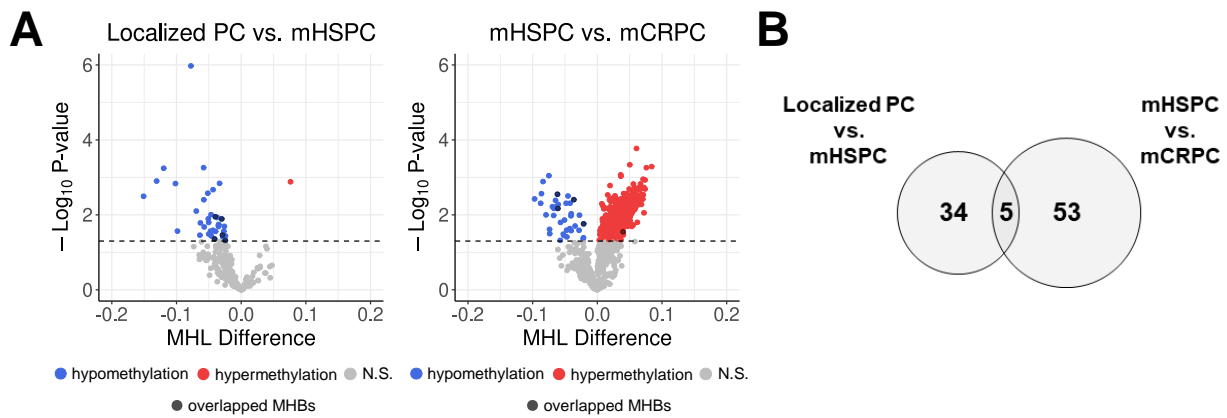
**Supplementary Figure S4: Median methylation of MHBs in positive and negative control regions.** The average methylation for each MHB within positive control (n=130) and negative control (n=16) regions across all patients (n=96). MHBs methylation haplotype blocks.

**A****B**

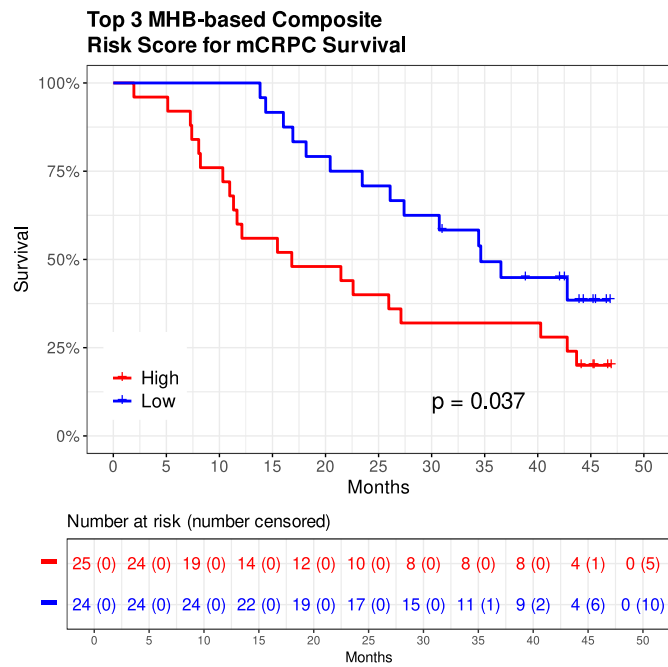
**Supplementary Figure S5: Distribution of the number of CpGs and bases found across the 1194 methylation haplotype blocks (MHBs) within the target regions. (A)** The distribution of the number of CpGs found in each MHB, which ranged from a minimum of 3 CpGs to a maximum of 137 CpGs. **(B)** The distribution of the number of bases found in each MHB, which ranged from a minimum of 5 bases to a maximum of 2100 bases. *MHBs* methylation haplotype blocks.



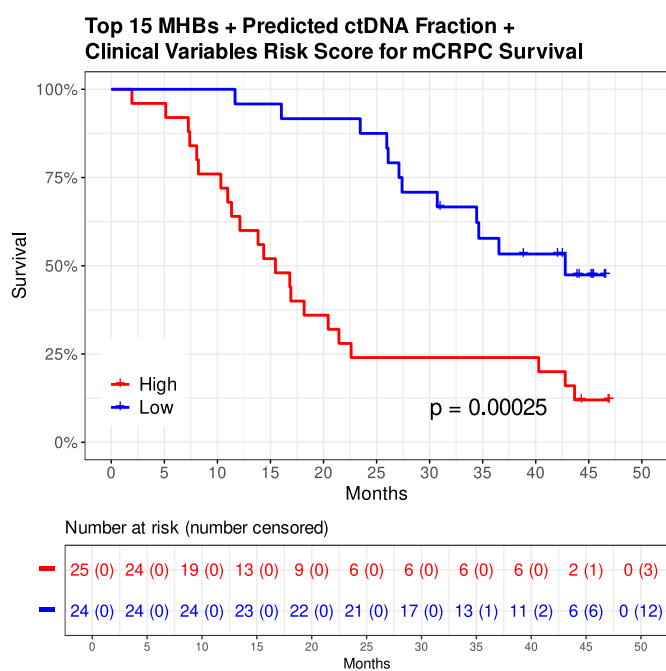
**Supplementary Figure S6: Distribution of the genic and CpG features across the 1194 MHBs within the target regions.** Genic features include 1 to 5 Kb regions upstream of the transcription start site (TSS), the promoters that are <1 Kb of the TSS, the 5'UTR, exons, introns, and 3'UTR. CpG features include CpG islands, CpG shores (2 Kb upstream/downstream from the end of a CpG island), CpG shelves (2 Kb upstream/downstream of the ends of the CpG shores) and inter-CGI regions (remaining non-CpG island regions). *MHBs* methylation haplotype blocks.



**Supplementary Figure S7: MHBs hypermethylated in localized PC are differentially methylated across the states of prostate cancer.** **(A)** Differential methylation of MHBs, with  $>0.05$  MHL in localized PC, when comparing localized PC to mHSPC and mHSPC to mCRPC. **(B)** Venn diagram depicting the significant MHBs, with  $>0.05$  MHL in localized PC, which are overlapping between the comparative analyses. *MHBs* methylation haplotype blocks, *PC* prostate cancer, *mHSPC* metastatic hormone sensitive prostate cancer, *mCRPC* metastatic castration resistant prostate cancer.

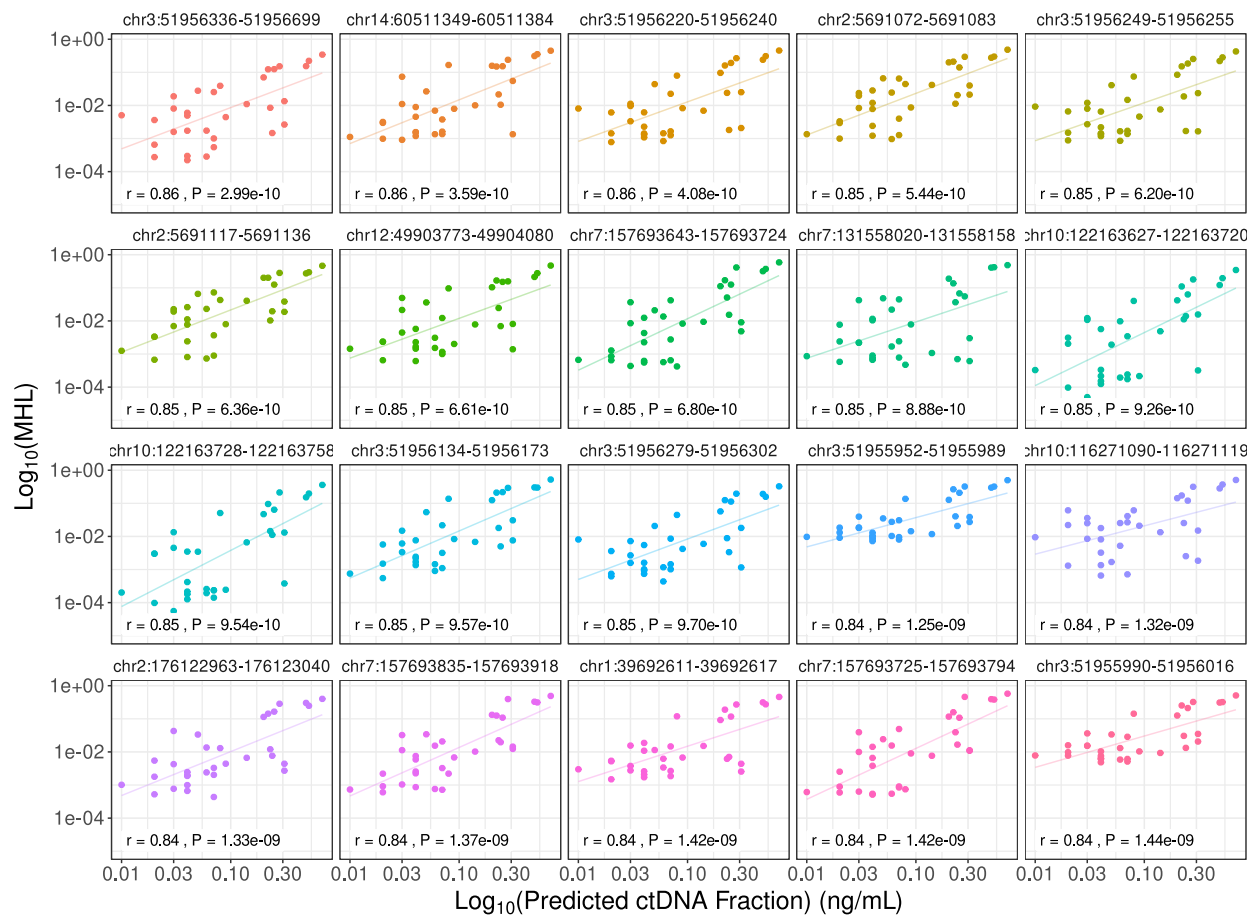


**Supplementary Figure S8: MHBs hypermethylated in localized PC are associated with mCRPC survival.** Kaplan-Meier plot showing mCRPC survival for patients stratified into high-risk and low-risk groups based on a 3 MHB-based composite risk score. *MHB* methylation haplotype block, *mCRPC* metastatic castration resistant prostate cancer.

**A****B**

**Supplementary Figure S9: ctDNA fraction, top MHBs, and clinical biomarkers are associated with mCRPC survival.** (A) Forest plot showing hazard ratios derived from multivariable Cox analysis. (B) Kaplan-Meier plot showing high-risk and low-risk groups for mCRPC survival based on composite score derived from predicted ctDNA fraction, 15 MHB-based composite score, and clinical biomarkers. *MHB* methylation haplotype block, *mCRPC* metastatic castration resistant prostate cancer.

### Correlation of Predicted ctDNA Fraction and MHL



**Supplementary Figure S10: ctDNA fraction is associated with mCRPC survival and highly correlated with MHL in select MHBs.** Plots demonstrating the correlation between MHBs and ctDNA fraction in the top 20 most correlated regions.